

Cite this: *Med. Chem. Commun.*, 2014, 5, 609

Multitarget-directed resveratrol derivatives: anti-cholinesterases, anti- β -amyloid aggregation and monoamine oxidase inhibition properties against Alzheimer's disease†

Long-Fei Pan, Xiao-Bing Wang, Sai-Sai Xie, Su-Yi Li and Ling-Yi Kong*

Considering the complex pathogenesis factors of Alzheimer's disease (AD), the multitarget-directed ligand strategy is expected to provide superior effects to fight AD, instead of the classic one-drug-one-target strategy. Resveratrol, exhibiting important properties against AD, was suggested to be used as a starting compound for the treatment of AD. Based on these reasons, a series of resveratrol derivatives were designed, synthesized and biologically evaluated. Among them, compound **6r**, exhibiting moderate cholinesterase inhibition activity (AChE, $IC_{50} = 6.55 \mu\text{M}$; BuChE, $IC_{50} = 8.04 \mu\text{M}$; $SI = 1.23$), significant inhibition of $A\beta_{42}$ aggregation (57.78%, at $20 \mu\text{M}$) and acceptable inhibitory activity against monoamine oxidases (MAO-A, $IC_{50} = 17.58 \mu\text{M}$; MAO-B, $IC_{50} = 12.19 \mu\text{M}$), was a potential anti-Alzheimer agent with balanced activities. Consequently, this study provided useful information for further development of resveratrol derivatives as multitarget-directed agents for AD therapy.

Received 7th December 2013
Accepted 14th February 2014

DOI: 10.1039/c3md00376k

www.rsc.org/medchemcomm

Introduction

Alzheimer's disease (AD), a progressive, chronic and fatal neurodegenerative disorder characterized by memory loss, cognitive impairment and decline in language, affects older people all over the world.¹ The pathology of AD includes cholinergic system dysfunction,² aggregated β -amyloid ($A\beta$) protein deposits,³ metal dyshomeostasis,⁴ τ -protein hyperphosphorylation,⁵ oxidative stress,⁶ neural loss and so on.⁷ These factors provide the bases for some hypotheses such as cholinergic hypothesis, one of the most classical hypotheses of AD, which suggests that the cognitive and memory deteriorations associated with AD are caused by the decline of acetylcholine (ACh). ACh can be degraded by two types of cholinesterases (ChEs), namely acetylcholinesterase (AChE) and butyrylcholinesterase (BuChE).⁸ The X-ray crystallographic structure of AChE reveals that it contains two binding sites: the catalytic active site (CAS) and the peripheral anionic site (PAS) connected by a deep, hydrophobic gorge.^{9,10} Generally, inhibitors that bind to either one of these sites can inhibit AChE. Current studies indicate that the PAS of AChE not only facilitates cholinergic transmission but also accelerates deposition and aggregation of $A\beta$.¹¹ In consideration of these reasons, dual

binding site acetylcholinesterase inhibitors (AChEIs) have become more promising in AD treatment. In a normal brain, AChE is more active than BuChE. However, as AD progresses, the activity of AChE gradually decreases, while that of BuChE is unchanged or increased.^{12,13} Thus, BuChE becomes a modulator to regulate ACh levels in cholinergic neurons. Due to the key role of BuChE, inhibition of both AChE and BuChE are beneficial for AD treatment.

In contrast to the cholinergic hypothesis, the amyloid hypothesis suggests that the aggregation of $A\beta$ leads to the formation of amyloid plaques, resulting in neuronal dysfunction in AD patients.^{14–16} $A\beta$ is a 39- to 43-residue peptide generated by the sequential cleaving of the amyloid precursor protein (APP) by β - and γ -secretases. $A\beta_{40}$ and $A\beta_{42}$ are the main isoforms of $A\beta$.¹⁷ $A\beta_{42}$ is the predominant form in amyloid plaques, having lower solubility and stronger neuronal toxicity than $A\beta_{40}$,¹⁸ therefore, the prevention of $A\beta_{42}$ formation or aggregation is currently another potential method for the treatment of AD.

It has been reported that monoamine oxidase (MAO), playing an important role in dopaminergic and serotonergic neurotransmitter systems, is a target for some multifactorial diseases.¹⁹ MAO is a flavoenzyme that catalyzes the deamination of amines and is responsible for the regulation and metabolism of major monoamine neurotransmitters. It has two isoforms named MAO-A and MAO-B.²⁰ MAO-A is involved in psychiatric conditions and depression, while MAO-B accelerates the oxidative deamination of neurotransmitters, resulting in enhanced production of free radicals thus causing oxidative

State Key Laboratory of Natural Medicines, Department of Natural Medicinal Chemistry, China Pharmaceutical University, 24 Tong Jia Xiang, Nanjing 210009, People's Republic of China. E-mail: cpu_lykong@126.com; Fax: +86-25-8327-1405; Tel: +86-25-8327-1405

† Electronic supplementary information (ESI) available. See DOI: 10.1039/c3md00376k

stress.²¹ As a result, selective inhibitors of MAO-A have been shown to be effective antidepressants, whereas MAO-B inhibitors are useful in neurodegenerative disorders such as AD.²² AD patients commonly have depressive symptoms which have been considered as risk factors for the development of AD. Therefore, dual inhibition of MAO-A and MAO-B, rather than only MAO-B, should contribute to AD therapy.²³

The pioneering strategy for treating AD aimed at a single target, such as ChEs, A β , transition metal ions or MAO. However, due to the complexity of AD, molecules that modulate the activity of a single target might not be sufficient to alter the progression of this disease. Thus, an efficient therapy is more likely to be achieved by drugs that incorporate several pharmacological effects into a single molecular entity.²⁴ This approach has been explored by many research groups and different multitarget-directed compounds have been reported in recent literature.^{25–27} In the light of this point, we are devoted to the study of multifunctional agents that not only merely inhibit ChEs, but also decrease A β aggregation and inhibit MAOs as well.

Resveratrol (*trans*-3,4',5-trihydroxystilbene) is a natural phenolic compound, present in many plants. *In vitro* and *in vivo* studies show that resveratrol has a number of biological activities including anti-inflammatory and antioxidant properties.^{28,29} Recently, many researchers have focused on its effects against AD, and demonstrated that resveratrol can inhibit A β self-aggregation, attenuate A β -induced toxicity, promote A β clearance and reduce senile plaques.^{30,31} Some studies also show that it has inhibitory effects on MAO activities.^{32,33} It could be concluded that resveratrol might be used as a starting compound in the design of multitargeted drugs for the treatment of AD. Hence, a series of resveratrol analogues, a 3,5-dimethoxy-*trans*-stilbene fragment linked with different amines by a 2- to 8-carbon spacer, were designed. Amino groups, protonated at physiological pH, could bind to the CAS of AChE.³⁴ The stilbene moiety could interact with the PAS *via* aromatic stacking interactions, meanwhile, inhibit A β self-aggregation and MAOs. Variable carbon spacers were designed to make the designed compounds fit the gorge and interact with both sites of AChE (Fig. 1). Herein, we report the design, synthesis, evaluation and molecular modeling of resveratrol derivatives as multitargeted compounds with anti-ChEs, anti-A β aggregation and MAO inhibition properties for the treatment of AD.

Results and discussion

Chemistry

The synthetic routes of resveratrol derivatives are shown in Scheme 1. The commercially available 3,5-dimethoxybenzylalcohol was reacted with phosphorus tribromide in the presence of pyridine to give compound 2, which was further refluxed in triethyl phosphate to provide compound 3 in 95% yield. 4-Hydroxybenzaldehyde reacted with different α,ω -dibromoalkanes in acetonitrile produced compounds 4a–g in 72–88% yields, and these compounds were then treated with *N*-methylbenzylamine and other amines in the presence of potassium carbonate to afford the key intermediates 5a–v in 73–84% yields. Finally, the target products 6a–v were obtained by the reaction of 3 with 5a–v through Wittig–Horner reaction in 40–54% yields.

Cholinesterase inhibitory activity

Inhibitory activities of the target compounds against AChE (from an electric eel) and BuChE (from equine serum) were tested by the spectrophotometric method of Ellman *et al.* with tacrine and galantamine as reference standards.^{35,36} The IC₅₀ values for AChE and BuChE inhibitions are summarized in Table 1. Most of the synthesized compounds showed higher inhibitory potency against ChEs than resveratrol, indicating that the introduction of amino group side chains could indeed increase the inhibitory capacity of the target compounds. To get the optimal linker length, compounds 6a–g were designed and synthesized. As shown in Fig. 2, compound 6e (AChE, IC₅₀ = 11.70 μ M; BuChE, IC₅₀ = 26.38 μ M) was the best inhibitor against AChE and BuChE, revealing that a six-carbon linker between the *trans*-stilbene moiety and amino group was the suitable length for ChE inhibition.

With the optimal length of the linker in hand, different terminal amines were introduced to explore the structure–activity relationship. It is worth noting that 6h (AChE, IC₅₀ = 1.56 μ M) was almost 8-fold more potent than 6e. It could be concluded that increased lipophilicity could lead to a rise in AChE inhibitory potency.^{37,38} In comparison with compounds 6e and 6h, inhibitory activities of 6i–n toward AChE were strongly decreased, revealing that the *N*-benzyl-*N*-ethyl group could completely fill the bottom of the AChE gorge and most of the

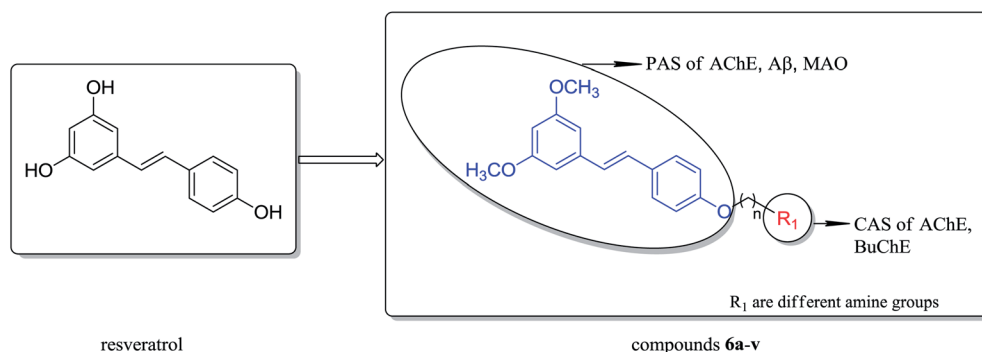
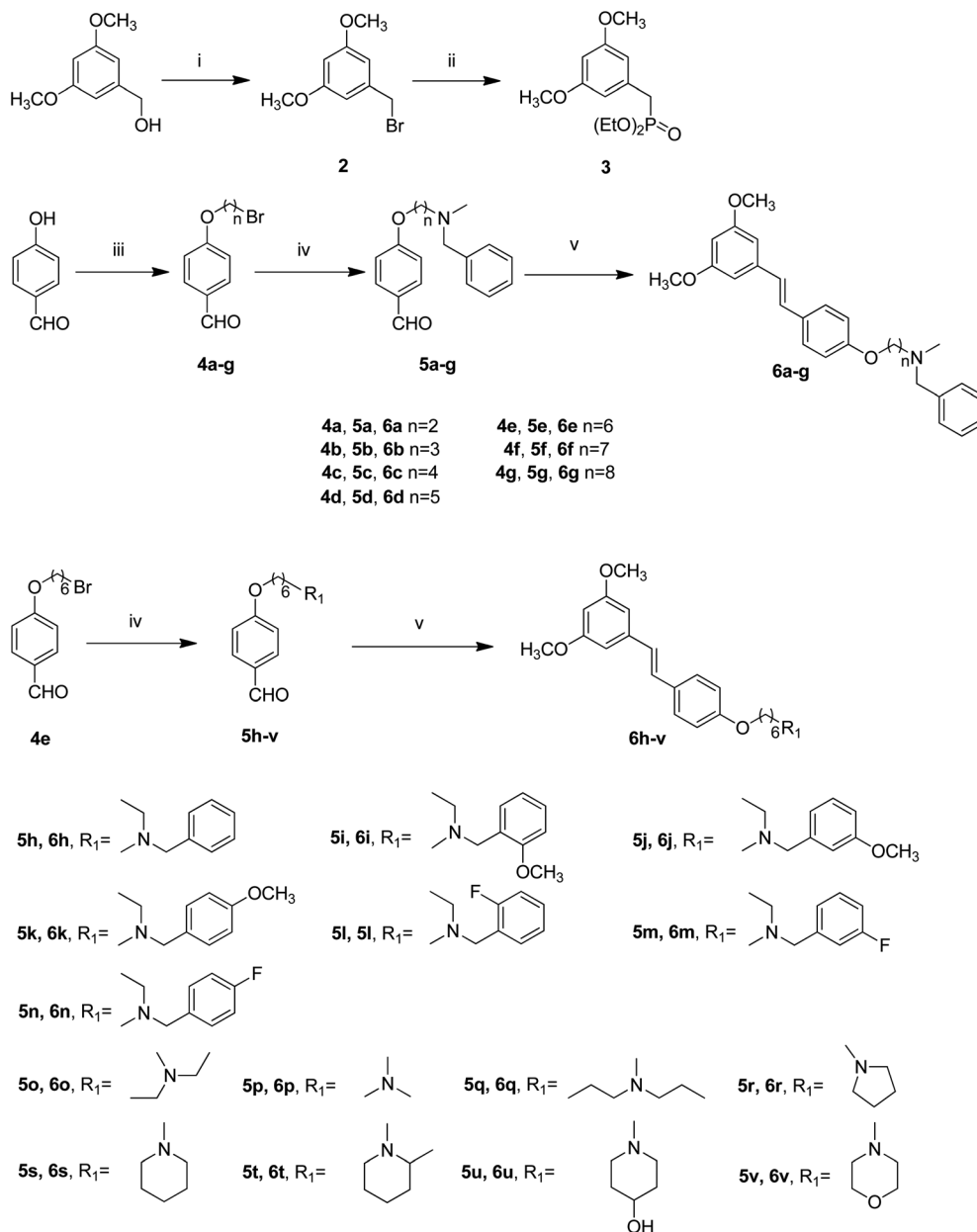


Fig. 1 Design strategy for resveratrol derivatives.



Scheme 1 Synthesis of resveratrol derivatives. Reagents and conditions: (i) PBr₃, pyridine, CH₂Cl₂, 0 °C to r.t., 4 h; (ii) triethyl phosphate, 160 °C, 4 h; (iii) α,ω-dibromoalkanes, K₂CO₃, acetonitrile, 40 °C, 4 h; (iv) NHR₁, K₂CO₃, acetonitrile, reflux, 8 h; (v) **3**, CH₃ONa, DMF, 0 °C, 0.5 h to r.t. 8 h.

changes on this part of the molecule were not allowed. With the exception of **6i** (IC₅₀ = 2.27 μM), compounds **6j–n** behaved similarly in the inhibition to BuChE, indicating that the *o*-methoxy group could stabilize the charged amino group through inductive and resonance effects.³⁹

Next, a phenyl ring was deleted from the amino group side chains with the aim to explore the differences between aliphatic amines (**6o–q**) and aromatic amines (**6e** and **6h**) against ChEs. The results showed that this modification did not remarkably affect the inhibitory potency. In addition, compared to **6o–q** with alkyl amine groups, compounds **6r–t** bearing cyclic amine groups demonstrated slightly better inhibitory activities against AChE, but no clear trend was observed for BuChE. As the lipophilicity increased, the activities against AChE of **6r–t** became stronger.

Interestingly, the inhibitory activity of compound **6q** was less than those of **6o** and **6p**, which might be attributed to the steric hindrance of the dipropylamine group. It also could be seen that compounds **6t** and **6u**, possessing oxygen atoms in the cyclic amino groups, exhibited weaker activities towards ChEs than those of **6r–t**. The result suggested that the electron-withdrawing effects of oxygen atoms might reduce the electronic density of amines and further impact on its protonation, thereby diminishing the interaction between the terminal nitrogen and ChEs.

Kinetic study of AChE inhibition

In order to gain insight into the mechanism of action of these derivatives on AChE, compound **6h** was selected for kinetic

Table 1 Inhibition of AChE, BuChE and self-induced A β ₄₂ aggregation activities of the synthesized compounds

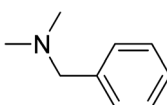
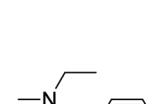
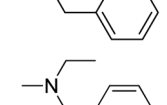
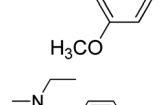
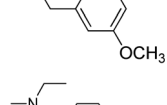
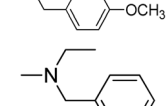
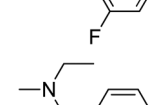
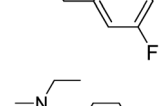
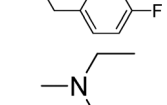
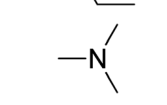
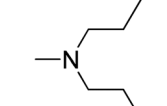
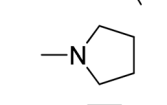
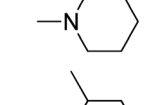
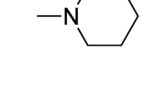
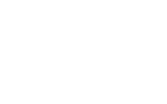
Compounds	R ₁	n	IC ₅₀ ^a (μM)		Selectivity index ^b	A β ₄₂ aggregation inhibition ^c (%)
			AChE	BuChE		
6a		2	79.30 ± 2.81	89.56 ± 3.54	1.13	26.14 ± 3.45
6b		3	58.06 ± 2.21	77.31 ± 2.76	1.33	46.40 ± 3.15
6c		4	60.89 ± 2.44	40.58 ± 1.63	0.67	44.72 ± 1.29
6d		5	39.16 ± 1.06	43.67 ± 2.01	1.13	36.40 ± 1.28
6e		6	11.70 ± 0.34	26.38 ± 1.28	2.25	49.79 ± 2.18
6f		7	23.40 ± 0.86	41.67 ± 1.89	1.78	43.57 ± 3.01
6g		8	26.50 ± 0.94	46.85 ± 2.07	1.77	47.20 ± 2.78
6h		6	1.56 ± 0.08	3.64 ± 0.06	1.69	53.49 ± 2.13
6i		6	54.93 ± 2.38	2.27 ± 0.09	0.04	64.53 ± 2.18
6j		6	71.53 ± 2.95	>100	>1.40	55.17 ± 2.34
6k		6	89.73 ± 4.12	>100	>1.11	53.25 ± 1.09
6l		6	86.61 ± 3.55	53.03 ± 2.18	0.61	29.55 ± 2.05
6m		6	77.85 ± 3.01	51.98 ± 1.89	0.67	28.25 ± 3.21
6n		6	92.30 ± 4.31	85.38 ± 3.42	0.93	37.28 ± 1.24
6o		6	4.15 ± 0.11	13.19 ± 0.62	3.18	40.33 ± 1.09
6p		6	8.19 ± 0.20	10.35 ± 0.49	1.26	42.85 ± 2.98
6q		6	12.09 ± 0.34	7.49 ± 0.12	0.61	41.45 ± 2.56
6r		6	6.55 ± 0.16	8.04 ± 0.22	1.23	57.78 ± 2.36
6s		6	5.02 ± 0.13	10.68 ± 0.19	2.14	54.00 ± 1.87
6t		6	4.07 ± 0.10	10.10 ± 0.32	2.48	52.10 ± 2.22

Table 1 (Contd.)

Compounds	R ₁	n	IC ₅₀ ^a (μM)		Selectivity index ^b	Aβ ₄₂ aggregation inhibition ^c (%)
			AChE	BuChE		
6u		6	17.20 ± 0.43	23.13 ± 0.90	1.34	42.55 ± 1.87
6v		6	24.35 ± 1.08	34.32 ± 1.18	1.41	42.16 ± 3.54
Tacrine			0.205 ± 0.02	0.052 ± 0.001	0.25	n.t. ^d
Galantamine			2.77 ± 0.15	13.61 ± 0.28	4.91	n.t. ^d
Resveratrol			165.24 ± 48	752.46 ± 87	4.55	68.51 ± 2.46
Curcumin			n.t. ^d	n.t. ^d	>1.26	52.21 ± 1.30

^a IC₅₀: 50% inhibitory concentration (mean ± SEM of three experiments). ^b Selectivity index = IC₅₀(BuChE)/IC₅₀(AChE). ^c Inhibition of self-mediated Aβ₄₂ aggregation and the measurements were carried out in the presence of 20 μM compounds (mean ± SEM of three experiments). ^d n.t. = not tested.

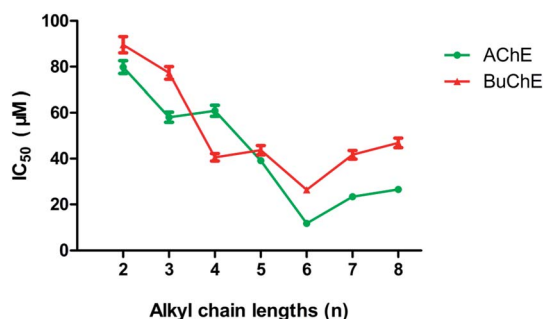
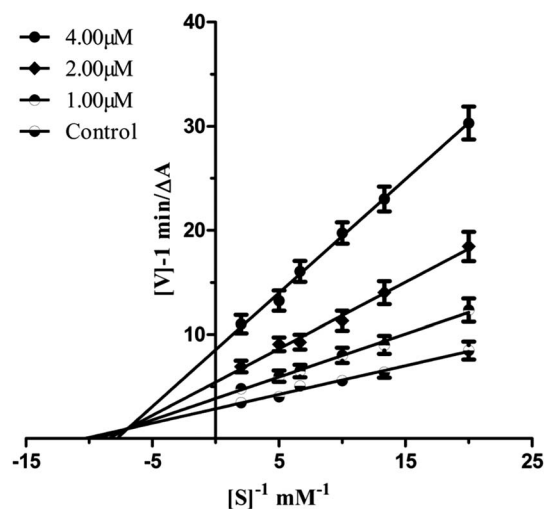


Fig. 2 Effects of alkyl chain lengths on anti-ChEs activities.

measurements because it showed the highest inhibitory activity against AChE. The graphical presentation of the steady-state inhibition data of **6h** for AChE is shown in Fig. 3. The results indicated that both slopes and intercepts were increased at increasing concentration of the inhibitor. This pattern indicated that compound **6h** was a mixed-type inhibitor, which could bind to the CAS as well as the PAS of AChE, demonstrating the rationality of our molecular design.

Molecular modeling studies

To further investigate the binding mode of the inhibitors, a molecular docking study was performed with the most active compound **6h** using Molecular Operating Environment (MOE) software package. The X-ray crystal structure of the AChE complex with bis(7)-tacrine (PDB code: 2CKM) was obtained from the Protein Data Bank. By analyzing as shown in Fig. 4(A) and (B), compound **6h** could perfectly fit into the gorge of AChE and simultaneously interact with the CAS and PAS of AChE. The phenyl ring substituted with methoxy groups was observed to bind to the PAS *via* π - π stacking interactions with the indole ring of Trp 279 with the distance of 4.16 Å. In the bottom of the gorge, the charged nitrogen of *N*-benzylethanamine could establish a cation- π interaction (4.63 Å) with the indole ring of Trp 84. The phenyl ring of *N*-benzylethanamine was bound to the CAS of

Fig. 3 Lineweaver–Burk plot for the inhibition of AChE by compound **6h**.

AChE, and stacked against the phenyl ring of Phe 330 and Trp 84 with the ring-to-ring distance of 3.75 and 3.73 Å, respectively. The docking results indicated that the **6h** was a mixed-type inhibitor of AChE, which were consistent with our kinetic analysis result.

Although there is little difference between compounds **6h** and **6i-n**, **6i-n** showed an obviously reduced anti-AChE activity compared with **6h**. Compounds **6i** and **6l** were selected as representative compounds to further explore the binding modes. From Fig. 4, it could be seen that both of them could bind to the CAS *via* the cation- π interaction with the indole ring of Trp 84, but no π - π stacking interactions were observed at the CAS and the PAS. These results might lead to the lower inhibitory capacity of **6i-n**.

Inhibition of Aβ₄₂ self-induced aggregation

The inhibition of self-induced Aβ₄₂ aggregation of these resveratrol derivatives was evaluated using a thioflavin-T based fluorometric assay.⁴⁰ Inhibition activities are listed in Table 1 as

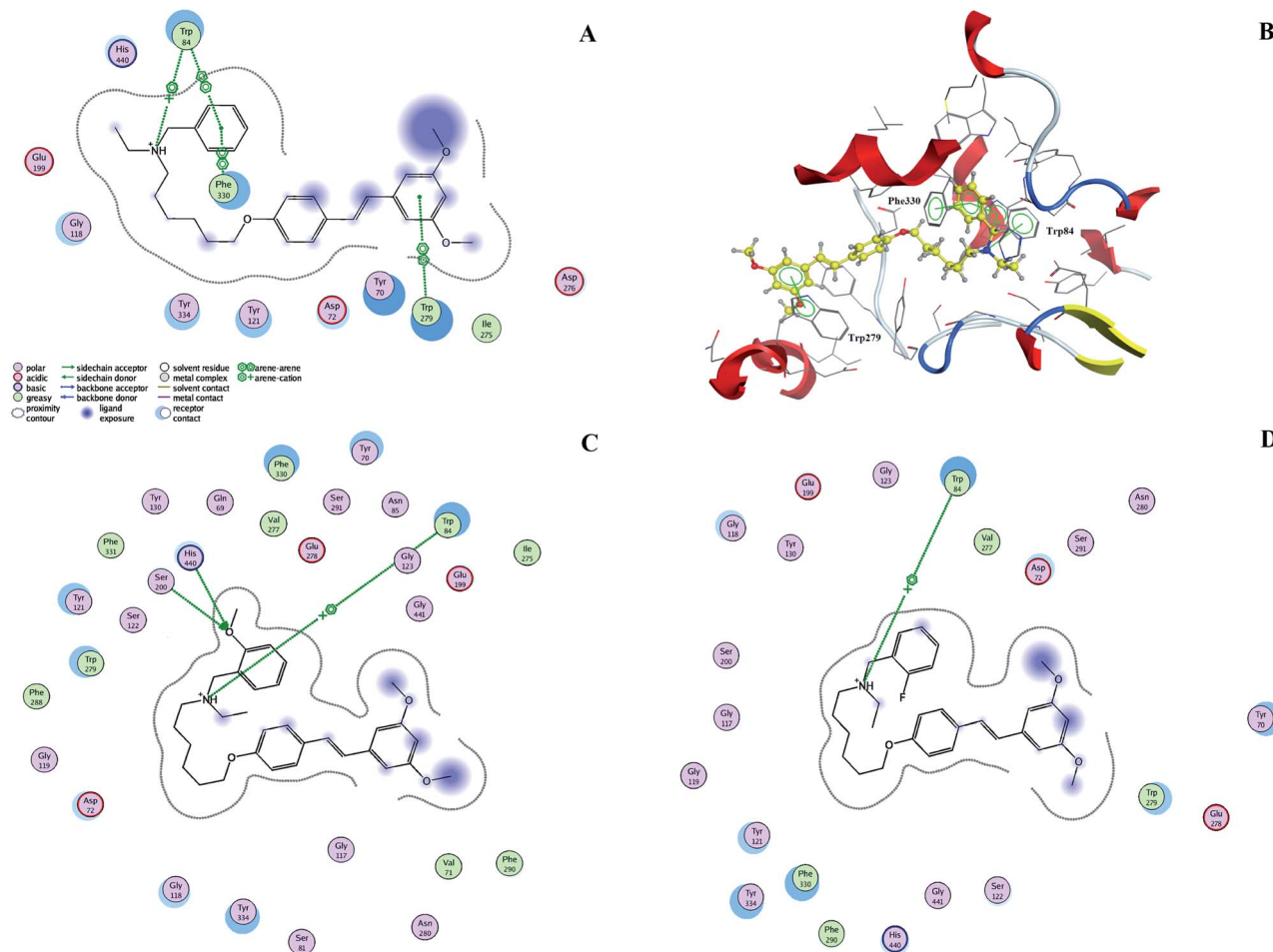


Fig. 4 Docking models of compounds **6h** (A and B), **6i** (C) and **6l** (D) with AChE generated with MOE.

inhibition ratios at a test concentration of 20 μM . Compared with the reference compounds, resveratrol (68.51%, at 20 μM) and curcumin (52.21%, at 20 μM), compounds **6h–k** and **6r–t** gave equal or better results, with inhibition ratios from 52.10% to 64.53%. Compound **6i** (64.53%, at 20 μM) was the strongest inhibitor among all these compounds. From the inhibition values of **6r–v** and **6o–q**, it was observed that compounds with cyclic monoamine groups had better inhibitory activities than those with chain monoamine groups. Compounds **6i–k** exhibited higher levels of inhibitory potency than compounds **6l–n**, revealing that electron-withdrawing substituents on the *N*-benzyl group might be beneficial to their activities against $\text{A}\beta_{42}$ aggregation.

Inhibition of MAO activity

To confirm the multipotent biological profile of all compounds, the activities of inhibiting the MAO-A and MAO-B were determined. The inhibitory activities were investigated by measuring the effects of each derivative on the production of hydrogen peroxide from *p*-tyramine, using the Amplex Red MAO assay, with iproniazid as the reference.⁴¹ Based on the screening data (Table 2), most of the compounds displayed slightly better inhibitory activities towards MAO-B than towards MAO-A.

MAO-A inhibition was very weak and no apparent structure–activity relationship existed, while the MAO-B inhibitory activity was relatively potent and related to the length of the alkyl chain. Among **6a–h** with the number of methylene varying from two to eight, compound **6b** with a 3-carbon spacer gave the best inhibition for MAO-B ($\text{IC}_{50} = 5.01 \mu\text{M}$). Shortening or extending the chain length could not improve the activity and it decreased as the number of carbon atoms varied from four to eight. On the other hand, it can be seen from the IC_{50} values that **6e** ($\text{IC}_{50} = 40.29 \mu\text{M}$) was more potent than **6h–n**, and a similar trend was observed for **6o–q**. Compounds bearing small amine groups exhibited a good MAO-B inhibitory potency, which revealed that steric hindrance of the substituted amino groups seemed to play a key role in the modulation of MAO-B inhibitory activity. Among the synthesized compounds, **6r** displayed good inhibition towards both MAO-A and MAO-B (MAO-A, $\text{IC}_{50} = 17.58 \mu\text{M}$; MAO-B, $\text{IC}_{50} = 12.19 \mu\text{M}$; SI = 0.70). Surprisingly, **6h**, the best ChE inhibitor, did not display potent inhibitions against MAOs (MAO-A, $\text{IC}_{50} = 89.65 \mu\text{M}$; MAO-B, $\text{IC}_{50} = 58.31 \mu\text{M}$). Compound **6r**, exhibiting remarkable MAO inhibitory activities, moderate inhibition of ChEs and significant inhibition of $\text{A}\beta_{42}$ aggregation, showed a balanced biological profile against all tested targets and was chosen for further evaluation.

Table 2 MAO inhibitory activities of the synthesized compounds

Compounds	IC ₅₀ ^a (μM)		Selectivity index ^b
	MAO-A	MAO-B	
6a	>100	89.04 ± 3.51	<0.89
6b	>100	5.01 ± 0.12	<0.50
6c	>100	34.61 ± 0.97	<0.35
6d	97.38 ± 8.6	16.19 ± 0.69	0.16
6e	90.35 ± 6.02	40.29 ± 1.77	0.45
6f	>100	63.77 ± 3.25	<0.64
6g	>100	>100	—
6h	89.65 ± 5.39	58.31 ± 0.41	0.65
6i	>100	>100	—
6j	>100	>100	—
6k	>100	>100	—
6l	>100	>100	—
6m	>100	97.51 ± 6.03	<0.97
6n	>100	>100	—
6o	33.09 ± 1.01	10.09 ± 0.43	0.31
6p	37.46 ± 1.74	7.52 ± 0.19	0.20
6q	89.43 ± 7.58	92.43 ± 5.39	1.03
6r	17.58 ± 0.76	12.19 ± 0.40	0.70
6s	29.83 ± 0.87	14.21 ± 0.57	0.48
6t	24.27 ± 0.91	16.29 ± 0.73	0.67
6u	>100	14.60 ± 0.64	<0.14
6v	>100	>100	—
Resveratrol	17.41 ± 0.51	29.37 ± 0.68	1.68
Iproniazid	6.58 ± 0.69	7.82 ± 0.41	1.19

^a IC₅₀: 50% inhibitory concentration (mean ± SEM of three experiments). ^b Selectivity index = IC₅₀ (MAO-B)/IC₅₀ (MAO-A).

SH-SY5Y neuroblastoma cell toxicity

On basis of the results above, the most potent compound **6r** was selected to further examine the potential toxicity effect on the human neuroblastoma cell line SH-SY5Y.^{22,42} After exposing the cells to this compound for 24 h, the cell viability was evaluated by the 3-(4,5-dimethylthiazol-2-yl)-2,5-diphenyltetrazolium (MTT) assay. The result indicated that **6r** did not show any significant effect on cell viability at 1–50 μM (1 μM: 97.0 ± 14.2%; 5 μM: 95.6 ± 13.4%; 10 μM: 94.4 ± 13.6%; 25 μM: 93.2 ± 10.5%; 50 μM: 90.8 ± 6.9%). This suggested that **6r** was nontoxic to SH-SY5Y cells and might be a suitable inhibitor for treating AD.

Conclusions

In conclusion, a series of resveratrol derivatives were designed, synthesized and evaluated as multitarget-directed anti-Alzheimer agents for their inhibitory activities on ChEs, Aβ₄₂ aggregation and MAOs. Most of those compounds could effectively inhibit ChEs than resveratrol. Enzyme kinetics and the molecular modeling studies revealed that the compounds could bind simultaneously to the CAS and the PAS of AChE. Compounds **6h–k** and **6r–t** exhibited inhibitory percentages similar to the reference compounds resveratrol and curcumin in inhibition of Aβ₄₂ aggregation assay. For MAO, most of the compounds showed slightly better inhibitory activities towards MAO-B than MAO-A. Among the tested compounds, compound

6h exhibited the best AChE (IC₅₀ = 1.56 μM) inhibitory activities, good inhibition of Aβ₄₂ aggregation (53.49%, at 20 μM), but displayed poor anti-MAOs activities. In contrast, compound **6r**, exhibiting significant inhibition of Aβ₄₂ aggregation, acceptable MAO inhibitory activities and moderate inhibition of ChEs, was a balanced inhibitor towards all tested targets for treating AD. In the cell toxicity assay, **6r** showed non-toxicity towards the SH-SY5Y cell at 1–50 μM. Altogether, the multifunctional effects of these resveratrol derivatives qualified them as potential anti-AD drug candidates, and **6r** could be a promising lead compound for further research.

Abbreviations

AD	Alzheimer's disease
ChEs	Cholinesterases
AChE	Acetylcholinesterase
BuChE	Butyrylcholinesterase
Aβ	β-Amyloid
CAS	Catalytic anionic site
PAS	Peripheral anionic site
AChEIs	Acetylcholinesterase inhibitors
APP	Amyloid precursor protein
MAO	Monoamine oxidase
MOE	Molecular operating environment
SI	Selectivity index

Acknowledgements

We acknowledge the financial support from the Program for Changjiang Scholars and Innovative Research Team in University (IRT1193), a Project Funded by the Priority Academic Program Development of Jiangsu Higher Education Institutions (PAPD).

References

- 1 S. F. Razavi, M. Khoobi, H. Nadri, A. Sakhteman, A. Moradi, S. Emami, A. Foroumadi and A. Shafiee, *Eur. J. Med. Chem.*, 2013, **64**, 252–259.
- 2 R. T. Bartus, R. L. Dean, B. Beer and A. S. Lippa, *Science*, 1982, **217**, 408–417.
- 3 J. Hardy and D. J. Selkoe, *Science*, 2002, **297**, 353–356.
- 4 H. Schugar, D. E. Green, M. L. Bowen, L. E. Scott, T. Storr, K. Böhmerle, F. Thomas, D. D. Allen, P. R. Lockman, M. Merkel, K. H. Thompson and C. Orvig, *Angew. Chem.*, 2007, **119**, 1746–1748.
- 5 L. Martin, X. Latypova, C. M. Wilson, A. Magnaudeix, M. L. Perrin, C. Yardin and F. Terro, *Ageing Res. Rev.*, 2013, **12**, 289–309.
- 6 D. J. Bonda, X. Wang, G. Perry, A. Nunomura, M. Tabaton, X. Zhu and M. A. Smith, *Neuropharmacology*, 2010, **59**, 290–294.
- 7 W. Huang, D. Lv, H. Yu, R. Sheng, S. C. Kim, P. Wu, K. Luo, J. Li and Y. Hu, *Bioorg. Med. Chem. Lett.*, 2010, **18**, 5610–5615.
- 8 T. Mohamed, J. C. Yeung, M. S. Vasefi, M. A. Beazely and P. P. Rao, *Bioorg. Med. Chem. Lett.*, 2012, **22**, 4707–4712.

- 9 M. Catto, L. Pisani, F. Leonetti, O. Nicolotti, P. Pesce, A. Stefanachi, S. Cellamare and A. Carotti, *Bioorg. Med. Chem. Lett.*, 2013, **21**, 146–152.
- 10 S.-S. Xie, X.-B. Wang, J.-Y. Li, L. Yang and L.-Y. Kong, *Eur. J. Med. Chem.*, 2013, **64**, 540–553.
- 11 H. Tang, H. T. Zhao, S. M. Zhong, Z.-Y. Wang, Z.-F. Chen and H. Liang, *Bioorg. Med. Chem. Lett.*, 2012, **22**, 2257–2261.
- 12 L. Yu, R. Cao, W. Yi, Q. Yan, Z. Chen, L. Ma, W. Peng and H. Song, *Bioorg. Med. Chem. Lett.*, 2010, **20**, 3254–3258.
- 13 C. Chianella, D. Gragnaniello, P. Maisano Delser, M. F. Visentini, E. Sette, M. R. Tola, G. Barbujani and S. Fuselli, *Eur. J. Clin. Pharmacol.*, 2011, **67**, 1147–1157.
- 14 T. Su, S. Xie, H. Wei, J. Yan, L. Huang and X. Li, *Bioorg. Med. Chem.*, 2013, **21**, 5830–5840.
- 15 E. Ozturan Ozer, O. U. Tan, K. Ozadali, T. Kucukkilinc, A. Balkan and G. Ucar, *Bioorg. Med. Chem. Lett.*, 2013, **23**, 440–443.
- 16 Y.-P. Chen, Z.-Y. Zhang, Y.-P. Li, D. Li, S.-L. Huang, L.-Q. Gu, J. Xu and Z.-S. Huang, *Eur. J. Med. Chem.*, 2013, **66**, 22–31.
- 17 S. Mandel, T. Amit, O. Bar-Am and M. B. H. Youdim, *Prog. Neurobiol.*, 2007, **82**, 348–360.
- 18 Y. He, P. F. Yao, S. B. Chen, Z. H. Huang, S. L. Huang, J. H. Tan, D. Li, L. Q. Gu and Z. S. Huang, *Eur. J. Med. Chem.*, 2013, **63**, 299–312.
- 19 I. Bolea, J. Juarez-Jimenez, C. de Los Rios, M. Chioua, R. Pouplana, F. J. Luque, M. Unzeta, J. Marco-Contelles and A. Samadi, *J. Med. Chem.*, 2011, **54**, 8251–8270.
- 20 N. Desideri, R. Fioravanti, L. Proietti Monaco, M. Biava, M. Yanez, F. Ortuso and S. Alcaro, *Eur. J. Med. Chem.*, 2013, **59**, 91–100.
- 21 H. Zheng, T. Amit, O. Bar-Am, M. Fridkin, M. B. Youdim and S. A. Mandel, *J. Alzheimer's Dis.*, 2012, **30**, 1–16.
- 22 C. Lu, Q. Zhou, J. Yan, Z. Du, L. Huang and X. Li, *Eur. J. Med. Chem.*, 2013, **62**, 745–753.
- 23 C. Lu, Y. Guo, J. Yan, Z. Luo, H.-B. Luo, M. Yan, L. Huang and X. Li, *J. Med. Chem.*, 2013, **56**, 5843–5859.
- 24 Y. Wang, F. Wang, J. P. Yu, F. C. Jiang, X. L. Guan, C. M. Wang, L. Li, H. Cao, M. X. Li and J. G. Chen, *Bioorg. Med. Chem. Lett.*, 2012, **20**, 6513–6522.
- 25 R. S. Keri, C. Quintanova, S. M. Marques, A. R. Esteves, S. M. Cardoso and M. A. Santos, *Bioorg. Med. Chem.*, 2013, **21**, 4559–4569.
- 26 A. S. Pithadia, A. Kochi, M. T. Soper, M. W. Beck, Y. Liu, S. Lee, A. S. DeToma, B. T. Ruotolo and M. H. Lim, *Inorg. Chem.*, 2012, **51**, 12959–12967.
- 27 S.-Y. Li, X.-B. Wang and L.-Y. Kong, *Eur. J. Med. Chem.*, 2013, **71**, 36–45.
- 28 M. Yanez, N. Fraiz, E. Cano and F. Orallo, *Biochem. Biophys. Res. Commun.*, 2006, **344**, 688–695.
- 29 J. F. Ge, J. P. Qiao, C. C. Qi, C. W. Wang and J. N. Zhou, *Neurochem. Int.*, 2012, **61**, 1192–1201.
- 30 C. Riviere, Y. Papastamoulis, P. Y. Fortin, N. Delchier, S. Andriamanarivo, P. Waffo-Teguo, G. D. Kapche, H. Amira-Guebalia, J. C. Delaunay, J. M. Merillon, T. Richard and J. P. Monti, *Bioorg. Med. Chem. Lett.*, 2010, **20**, 3441–3443.
- 31 C. Riviere, T. Richard, L. Quentin, S. Krisa, J. M. Merillon and J. P. Monti, *Bioorg. Med. Chem.*, 2007, **15**, 1160–1167.
- 32 M. Yanez, N. Fraiz, E. Cano and F. Orallo, *Biochem. Biophys. Res. Commun.*, 2006, **344**, 688–695.
- 33 Y. N. Han, S. Y. Ryu and B. H. Han, *Arch. Pharm. Sci. Res.*, 1990, **13**, 132–135.
- 34 R.-S. Li, X.-B. Wang, X.-J. Hu and L.-Y. Kong, *Bioorg. Med. Chem. Lett.*, 2013, **23**, 2636–2641.
- 35 G. L. Ellman, K. D. Courtney, V. Andres Jr and R. M. Featherstone, *Biochem. Pharmacol.*, 1961, **7**, 88–95.
- 36 F. C. Meng, F. Mao, W. J. Shan, F. Qin, L. Huang and X.-S. Li, *Bioorg. Med. Chem. Lett.*, 2012, **22**, 4462–4466.
- 37 V. Tumiatti, M. Rosini, M. Bartolini, A. Cavalli, G. Marucci, V. Andrisano, P. Angeli, R. Banzi, A. Minarini, M. Recanatini and C. Melchiorre, *J. Med. Chem.*, 2003, **46**, 954–966.
- 38 L. Piazzi, F. Belluti, A. Bisi, S. Gobbi, S. Rizzo, M. Bartolini, V. Andrisano, M. Recanatini and A. Rampa, *Bioorg. Med. Chem.*, 2007, **15**, 575–585.
- 39 L. Piazzi, A. Cavalli, F. Belluti, A. Bisi, S. Gobbi, S. Rizzo, M. Bartolini, V. Andrisano, M. Recanatini and A. Rampa, *J. Med. Chem.*, 2007, **50**, 4250–4254.
- 40 A. A. Reinke and J. E. Gestwicki, *Chem. Biol. Drug Des.*, 2007, **70**, 206–215.
- 41 F. Chimentì, D. Secci, A. Bolasco, P. Chimentì, B. Bizzarri, A. Granese, S. Garradori, M. Yáñez, F. Orallo, F. Ortuso and S. Alcaro, *J. Med. Chem.*, 2009, **52**, 1935–1942.
- 42 H. Zheng, M. B. Youdim and M. Fridkin, *J. Med. Chem.*, 2009, **52**, 4095–4098.